Belgium

Computational Physics: Biphenylene

Kobe Van Daele, Lukas Herygers, and Yarno Omblets
(Dated: December 5, 2025)

Computational study of Biphenylene under various degrees of tensile and compressive strains. This study focuses on the electronic band structure and DOS with strain up to ±4%. This study does not confirm bandgap creation under the most extreme stresses calculated.

I. INTRODUCTION

The biphenylene network (BPN) is a two-dimensional carbon allotrope consisting of four-, six-, and eight-membered rings connected through C-C bonds (See Figure 5). In this work we present a computational study of BPN using the density-functional theory (DFT) code Quantum Espresso together with the PBE exchange-correlation functional. All calculations were performed using a self-consistent-field (SCF) energy convergence threshold of 10^{-8} Ry, Marzari–Vanderbilt (MV) smearing, and without spin polarization.

We begin this study with a hydrostatic pressure test and th<e construction of energy-area curves $E(A)$[1], both with and without externally applied pressure.
Furthermore, we investigate the influence of mechanical strain on the electronic band structure, as well as the electron densities due to chemical bonding. Finally, we take a look at the phonon band structure in a frozen phonon calculation.

II. E(A) CURVE

We began this study by performing a series of convergence tests to ensure the numerical reliability of our calculations. From these tests we determined that an energy cutoff of $ecutwfc = 80$ Ry and a charge-density cutoff of $ecutrho = 480$ Ry were sufficient for well-converged total energies. A dense $26 \times 26 \times 1$ k-point mesh[2] was used to sample the Brillouin zone. The out-of-plane lattice parameter was fixed to $c = 30$ Å, which in convergence testing proved to provide adequate vacuum separation for a strictly two-dimensional system.

With these parameters we computed the $E(A)$ curve (Figure 1) and subsequently performed a full tensor relaxation, converging the residual in-plane stress to below 0.1 kbar. The optimal area of the plane is estimated to be 16.9 Å^2 for a non-stressed lattice, Figure 1 also shows the clear parabolic behavior of the Energy-Area relation as is expected from theory. After relaxation we then receive new coordinates for the atoms in our cell and we repeat this process for every strained input file we use later in this work (See Figure 7). This step is of the utmost importance!

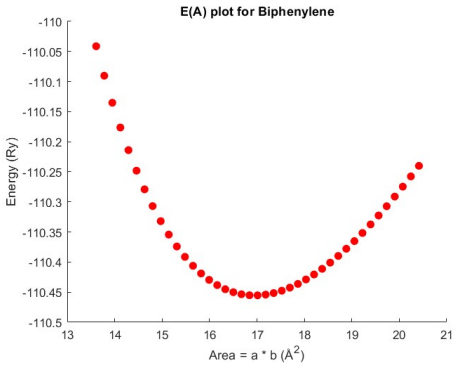

FIG. 1: E(A) curve, unstrained BPN, ecutwfc = 80Ry, ecutrho = 480Ry, c=fixed, and k-mesh 26x26x1.

III. ELECTRONIC BAND STRUCTURE

This section analyzes the effects of uniaxial (yy and xx) and biaxial (xy) strain on the electronic band structure of BPN.

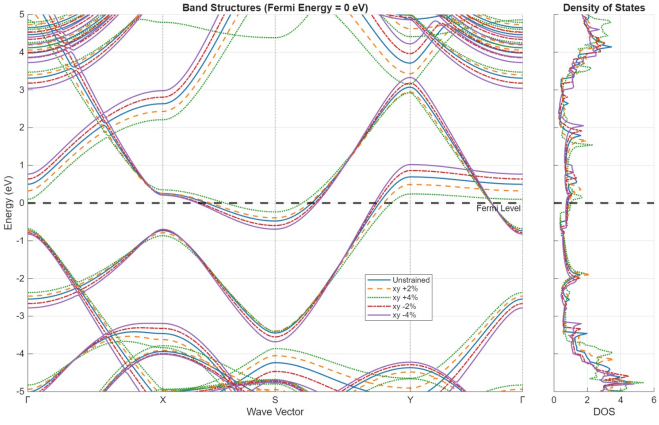

FIG. 2: Electronic band structure and DOS under XY type strain for five different conditions: $-4\%, -2\%, 0\%, +2\%, +4\%$. The Fermi level is set to 0 eV. Figure prepared in Matlab.

Figure 2 illustrates the coupling between mechanical deformation and electronic response. In the energy range from −5 eV to 5 eV, the density of states' overall trend is that it increases with energy (in 3D $DOS \propto E^{1/2}$), but the DOS shows pronounced features such as multiple

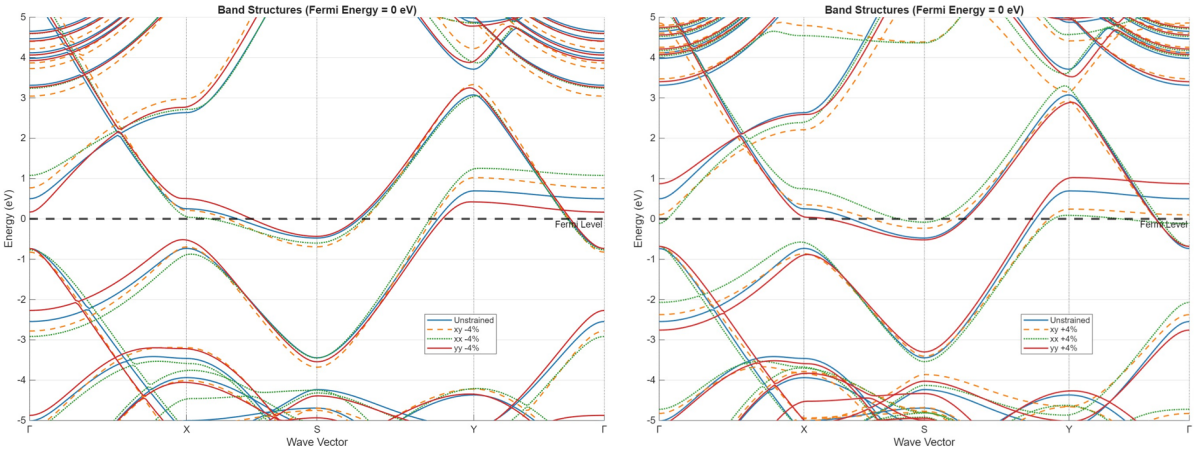

FIG. 3: Electronic band structures under the most extreme compressive (left) and tensile (right) strains for all strain types (xx, yy, xy), compared to the unstrained structure.

van Hove peaks originating from the flatter regions in the bandstructure. Here, only the DOS for xy strain is shown, other strain types have been calculated and exhibit similar trends (see Figure 4). Although the band structure was calculated from -23eV to 5.5eV, we focus here on the first 5 eV, which are most relevant for electronic and optical applications and are cleaner to visualize.

When plotting the most extreme compressive and tensile strains of all types (yy, xx and xy)onto one plot we get Figure 3. Noteworthy, in Figure 3 at the high-symmetry point ($Y \rightarrow \Gamma$), bands shift approximately in parallel under all types of strain. The Fermi level intersects multiple bands near the S point, confirming the presence of electronic states at E_F and indicating that BPN is metallic (or at least semi-metallic). The absence of the Fermi energy crossing all k-points reflects its anisotropic electronic behavior.

Even under +4% tensile strain, no bandgap opens, however extrapolation suggests that a gap might form at higher strains along the xx direction (keep in mind that higher strains are very unrealistic, by that point the material would probably fail).

The band curvature near the Fermi level is steep, particularly under compressive strain (-4%) for all types except yy, implying a reduced electron effective mass and higher carrier mobility. The highly dispersive bands also indicate strong orbital overlap and delocalization, consistent with the extended π-conjugation of the carbon network [3].

Interestingly, the low-energy bands under xy strain resemble those under xx strain more than yy strain. This suggests that strain along the xx direction dominates the low-energy electronic response. This anisotropy probably arises from the different types of carbon-carbon bonds being stretched (See Figure 4 for a visual of the structure). We therefore speculate that yy strain which primarily elongates the longer, C_8 rings changes the orbital overlap less significantly than the xx strain which stretches the smaller C_6 and C_4 rings. These bonds are π-conjugations and have a strong, sensitive orbital overlap. In Tight Binding method -a method where band energies arise from electrons "hopping" between atomic orbitals influenced by bond lengths and angles (2),(3)- this results in a significant shift in the band structure. Since biaxial strain includes the xx component, its electronic response is dominated by this more sensitive/profound change in orbital overlap.

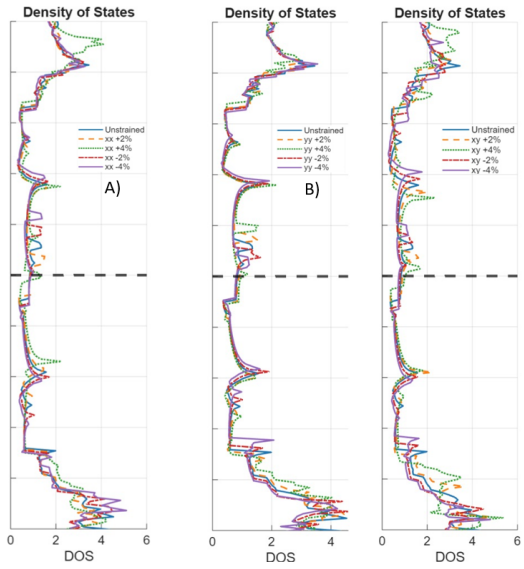

FIG. 4: DOS under xx, yy and xy type strain for five different conditions: $-4\%, -2\%, 0\%, +2\%, +4\%$. The Fermi level is set to 0 eV and the energy axis goes from $-5eV$ to $+5eV$. Figure prepared in Matlab.

Finally, the DOS shapes under different strain intensities remain similar near the Fermi level, shifting approxi-

mately in parallel (upwards for tensile strain for yy and downwards for xy/xx), following the same connection as discovered in the bandstructure. Deviations from the original unstrained shape become more noticeable at energies further from E_F, indicating that low-energy electronic availability is minimally affected, whilst the shape of the DOS changes significantly in the higher energy regions. The DOS-structures that were calculated up to 20 eV showed that beyond approximately 12 eV, the peaks again start to shift in a parallel fashion due to the flatness of the higher energy bands and the parallel offset that is created due to the stress condition.
We can also verify the calculation by confirming that tensile and compressive strain produce opposite band shifts, since stretching reduces orbital overlap while compression increases it.

IV. ELECTRON DENSITIES BPN

In this section we discuss the unstrained BPN's electron densities.

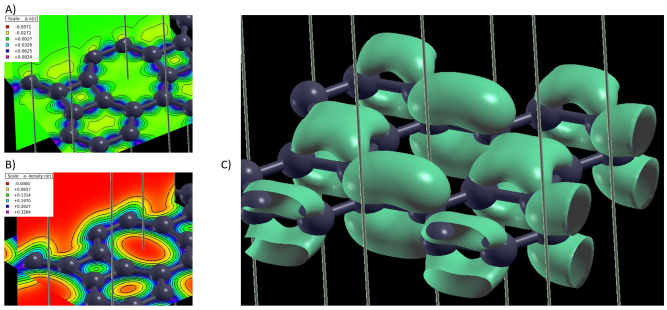

FIG. 5: A) Electron-density difference of BPN. The stick–ball structure is shown in the xy-plane (with the x-axis pointing left–up). The xy-plane lies in the molecular sheet, while the zy-plane cuts perpendicularly through a benzene ring. B) Total electron density in the same orientation as A). C) Isosurface of a selected Kohn–Sham wavefunction visualizing the π-bonding character that is partly obscured in A) and B).

Figure 5 provides several complementary visualizations of the electronic structure of BPN. As expected for a covalently bonded carbon network, regions of enhanced electron density appear between neighboring C atoms. This is most clearly visible in panel A), where the electron-density difference is plotted. The positive contours of $\Delta n(\mathbf{r})$ lie primarily in the bond regions, showing how the electron density is redistributed relative to the reference state, consistent with the formation of bonds. Because BPN contains aromatic rings, the system is expected to exhibit delocalized π electrons above and below the plane of each ring. This behavior is slightly visible in the zy-plane slice of panel A): the contour matches that from benzene (4), where the π electron cloud forms a "hollow-cushion" profile. However, due to the stronger σ-bonds, these are overshadowed.
To visualize these π-states, panel C) shows an isosurface of a selected Kohn–Sham wavefunction. In this particular visualization only the wavefunctions associated with the C_4 rings were selected, other delocalized states are present in the electronic structure but are not shown here.

V. FROZEN PHONON CALCULATIONS

The phonon band structure describes how vibrational frequencies vary throughout the Brillouin zone and therefore reveals the allowed vibrational modes. In analogy to the electronic case, one can also construct a phonon DOS, which provides the number of vibrational states available at each energy.

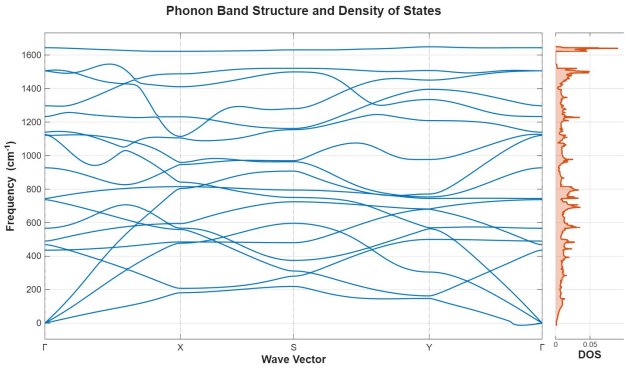

FIG. 6: The phonon band structure (left) and the phonon DOS (right) of unstrained BPN.

In a single-layer, the phonon dispersion has three acoustic and $3N-3$ optical branches, with N the amount of atoms in a unit cell. For BPN, we expect the LA (Longitudinal Acoustic), TA (Transverse Acoustic) and ZA (out-of-plane acoustic) modes to appear, all starting from zero frequency near the Γ-point, as needed for a stable and unconstrained structure. Figure 6 shows these acoustic branches. The sound velocities can be found from the slopes of LA and TA modes near Γ.
A small amount of negative frequency in the DOS is still present. Since real phonon frequencies cannot be negative, this indicates most likely a numerical issue. The ZA acoustic branch also does not show a clearly quadratic dispersion near Γ, although a free and unstrained 2D lattice is expected to show $\omega_{ZA} \propto q^2$. The precision can be the cause of this behavior [4], however, several other factors may influence the curvature of the ZA mode. This includes: the vacuum spacing (the c-axis in this calculation was smaller), residual in-plane stress, the pseudopotential, and the K-point mesh density. The existence of **small** negative frequencies indicates numerical noise in the tiny force constant around Γ, which can affect both the soft mode and ZA curvature. Finally, the many high-frequency optical branches are consistent with the numerous C-C bonds present in the BPN.

VI. SUPPLEMENTARY VISUALIZATION

A showcase on the effect of strain on the atom coordinates in a C_6 ring within the BPN structure.

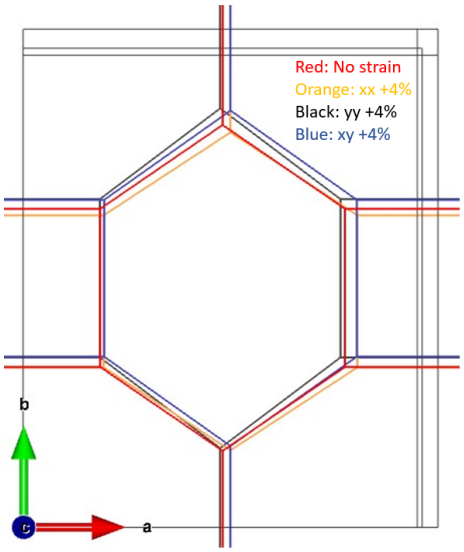

FIG. 7: Showcasing of the changing lattice under tensile strains: xx= +4%, yy= +4%, xy= +4% and unstrained.

VII. BIBLIOGRAPHY

- (1) Fan, Q., Yan, L., Tripp, M. W., Krejčí, O., Dimosthenous, S., Kachel, S. R., Chen, M., Foster, A. S., Koert, U., Liljeroth, P., Gottfried, J. M. (2021). Biphenylene network: A nonbenzenoid carbon allotrope. Science, 372(6544), 852–856. https://doi.org/10.1126/science.abg4509

- (2) Bachelor's thesis: The amphoteric doping of single-walled carbon nanotubes, Kobe Van Daele

- (3) Wallace, P. R. (1947). The band theory of graphite. Physical Review, 71(9), 622–634. https://doi.org/10.1103/PhysRev.71.622

- (4) Ninković, D. B., Blagojević, J. P., Hall, M. B., Zarić, S. D. (n.d.). Overlaid electrostatic potentials for benzene–benzene and cyclohexane–benzene [Figure]. ResearchGate. https://www.researchgate.net/figure/Overlaid-electrostatic-potentials-for-benzene-benzene-and-cyclohexane-benzene_fig3_339639196

---

[1] Because BPN is a two-dimensional material, the energy is plotted as a function of area rather than volume.
[2] All calculations were performed on the HPC cluster of the University of Antwerp.
[3] Type-II Dirac cones were reported in (1), but these lie outside the k-vector region considered here and are not observed in our calculations.
[4] A higher precision calculation with the hardware available to us was not possible.